

## Supporting Information

### Electronic engineering and oxygen vacancy modification of $\text{La}_{0.6}\text{Sr}_{0.4}\text{FeO}_{3-\delta}$ perovskite oxide by low-electronegativity sodium doping for efficient reversible $\text{CO}_2/\text{CO}$ fueled solid oxide cells

Wanbin Lin<sup>a</sup>, Yihang Li<sup>b\*</sup>, Manish Singh<sup>c</sup>, Huibin Zhao<sup>a</sup>, Rui Yang<sup>a</sup>, Pei-Chen Su<sup>d\*</sup>, Liangdong Fan<sup>a\*</sup>

<sup>a</sup> Department of New Energy Science & Technology, College of Chemistry and Environmental Engineering,  
Shenzhen University, Shenzhen 518060, Guangdong, China.

<sup>b</sup> Interdisciplinary Research Center of Smart Sensors, Academy of Advanced Interdisciplinary Research, Xidian  
University, Xi'an 710026, China.

<sup>c</sup> Department of Metallurgical and Materials Engineering, Indian Institute of Technology Patna, Bihta, Bihar  
801106, India

<sup>d</sup> School of Mechanical and Aerospace Engineering, Nanyang Technological University, 50 Nanyang Avenue,  
Singapore 639798, Singapore.

\*Corresponding Authors: Email: [fanld@szu.edu.cn](mailto:fanld@szu.edu.cn); [liyihang@xidian.edu.cn](mailto:liyihang@xidian.edu.cn); [peichensu@ntu.edu.sg](mailto:peichensu@ntu.edu.sg)

Totally 18 figures and 5 tables

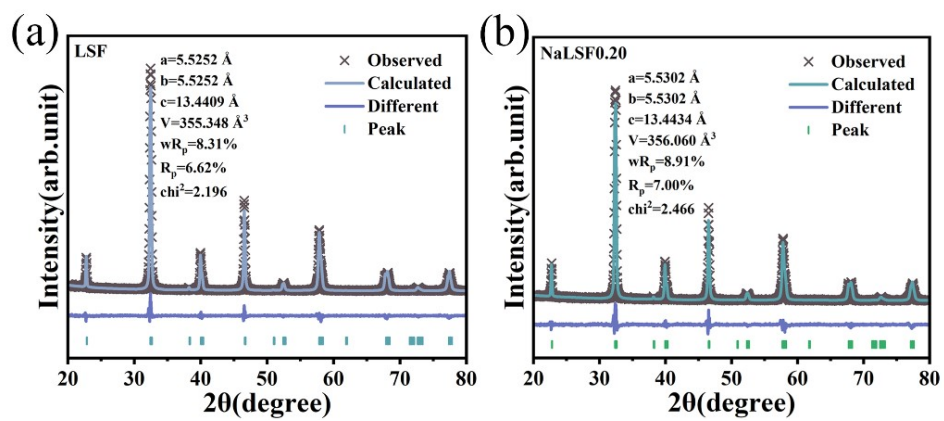


**Fig. S1.** The profiles of XRD refinement of a) LSF and b) NaLSF0.20 powders.

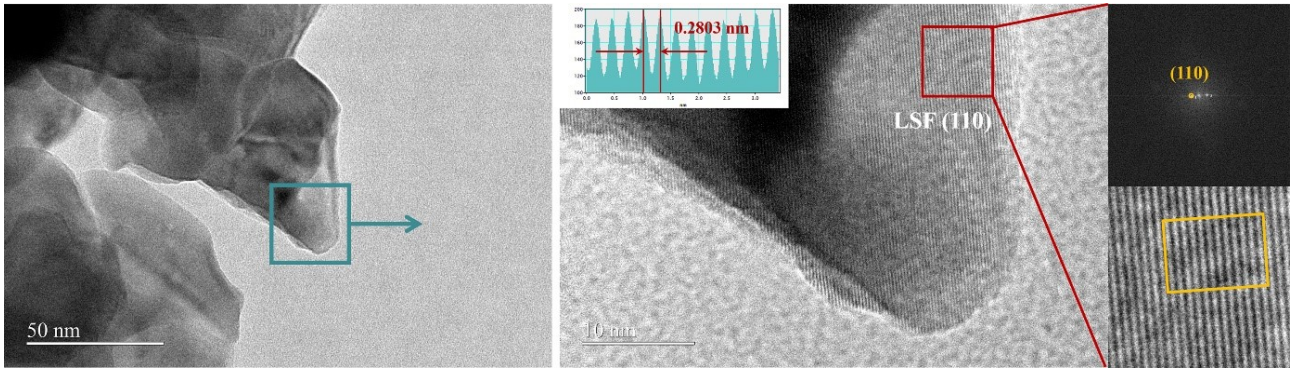


**Fig. S2.** HR-TEM microscope of LSF powder.

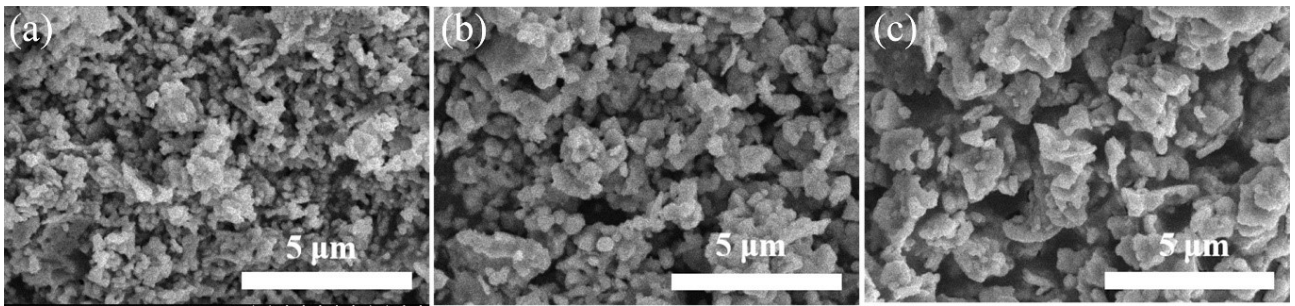


**Fig. S3.** The SEM of microscope structure of a) LSF, b) NaLF0.10, and c) NaLSF0.20 powders.

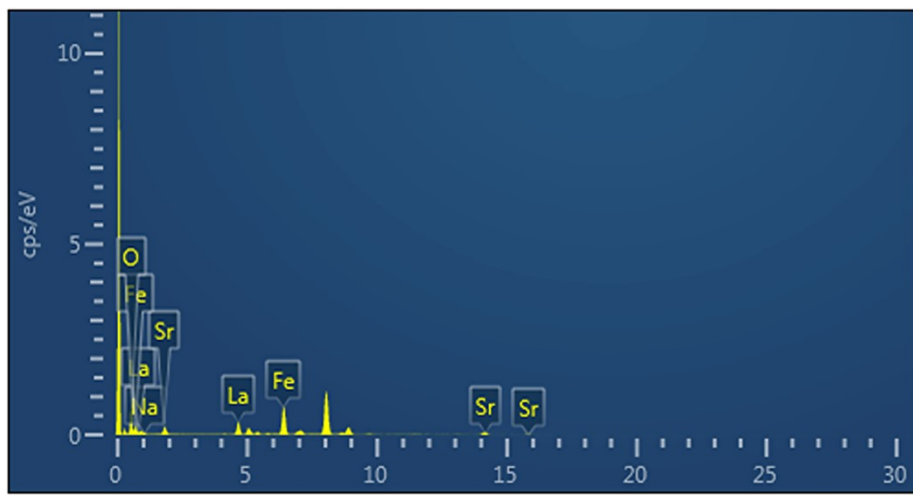


**Fig. S4.** Elements' content obtained by EDX.

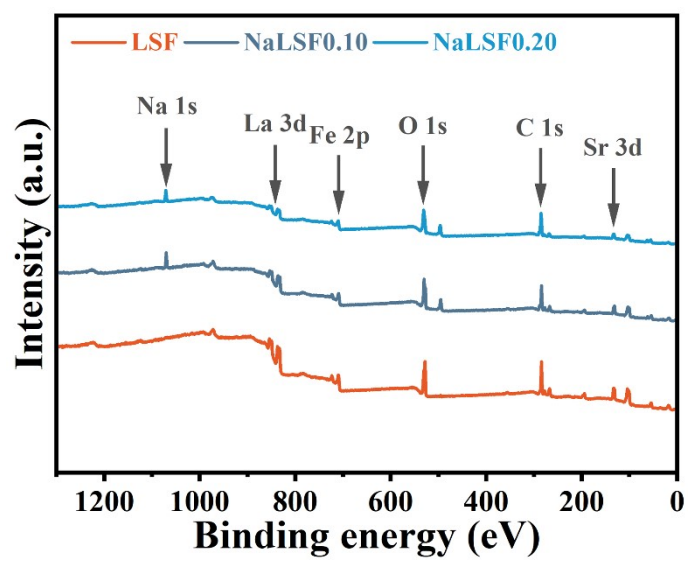
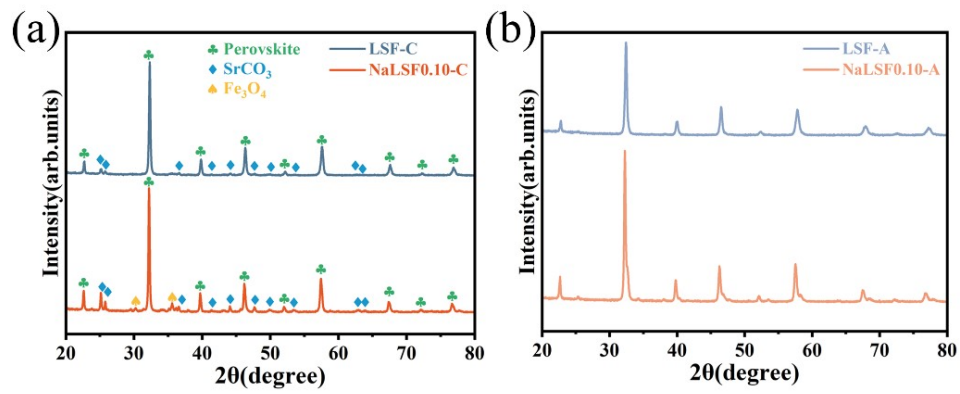
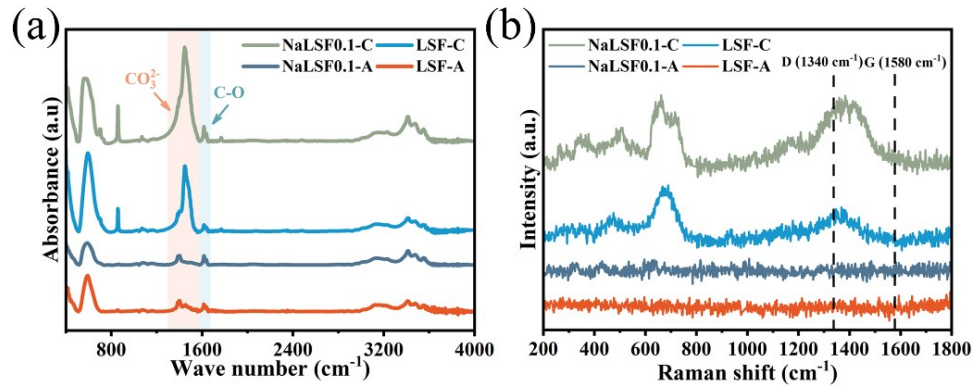


Fig. S5. XPS full survey spectra of all powders.



**Fig. S6.** Physical properties of LSF and NaLSF0.10: a) XRD patterns after sintered at 50% CO-CO<sub>2</sub> atmosphere, b) XRD patterns of both samples in Figure 4a after successively sintered under air atmosphere for 10 h.



**Fig. S7.** Chemical properties of LSF and NaLSF0.10 after sintered at 50% CO-CO<sub>2</sub> atmosphere and air atmosphere for 10 h: a) the Fourier infrared spectra, b) Raman spectra.



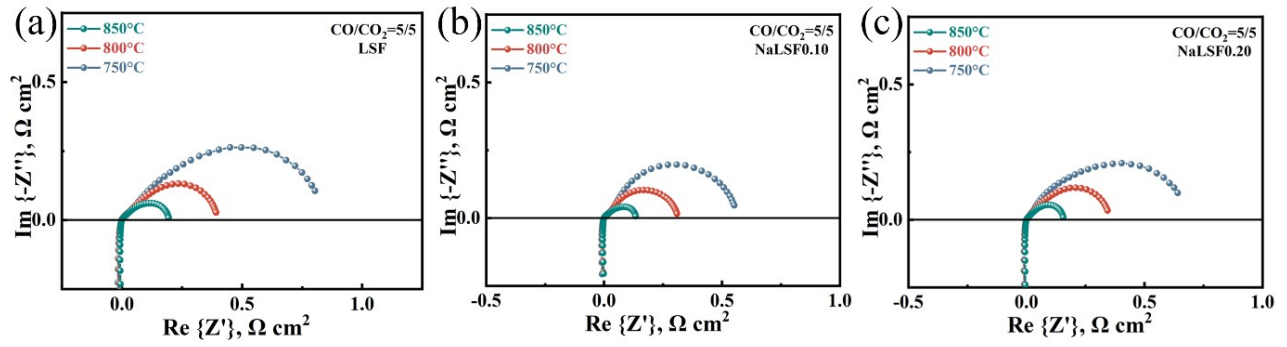


**Fig. S8.** EIS curves of symmetrical cells with a) LSF, b) NaLSF0.10, and c) NaLSF0.20 cathodes from 750 °C to 850 °C at 50% CO-CO<sub>2</sub> atmosphere.

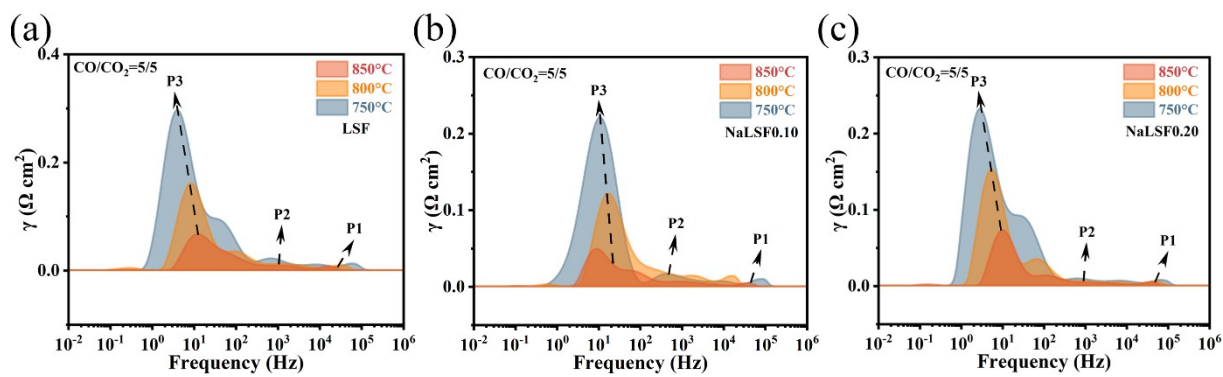


**Fig. S9.** DRT curves of symmetrical cells with a) LSF, b) NaLSF0.10, and c) NaLSF0.20 cathodes from 750 °C to 850 °C at 50% CO-CO<sub>2</sub> atmosphere.

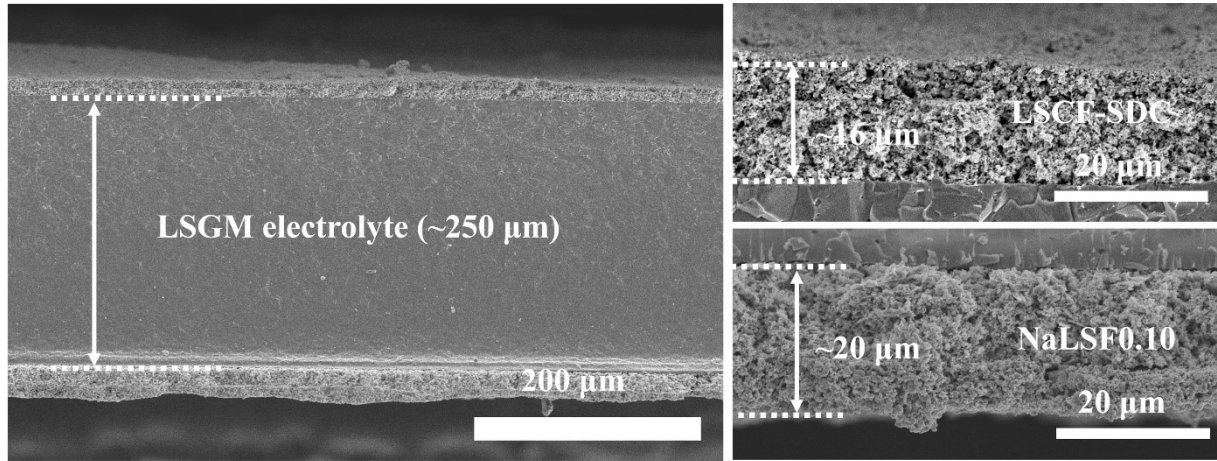


**Fig. S10.** SEM images of the cross-sectional of SOECs before the test with NaLSF0.10 cathode and LSCF-SDC anode.

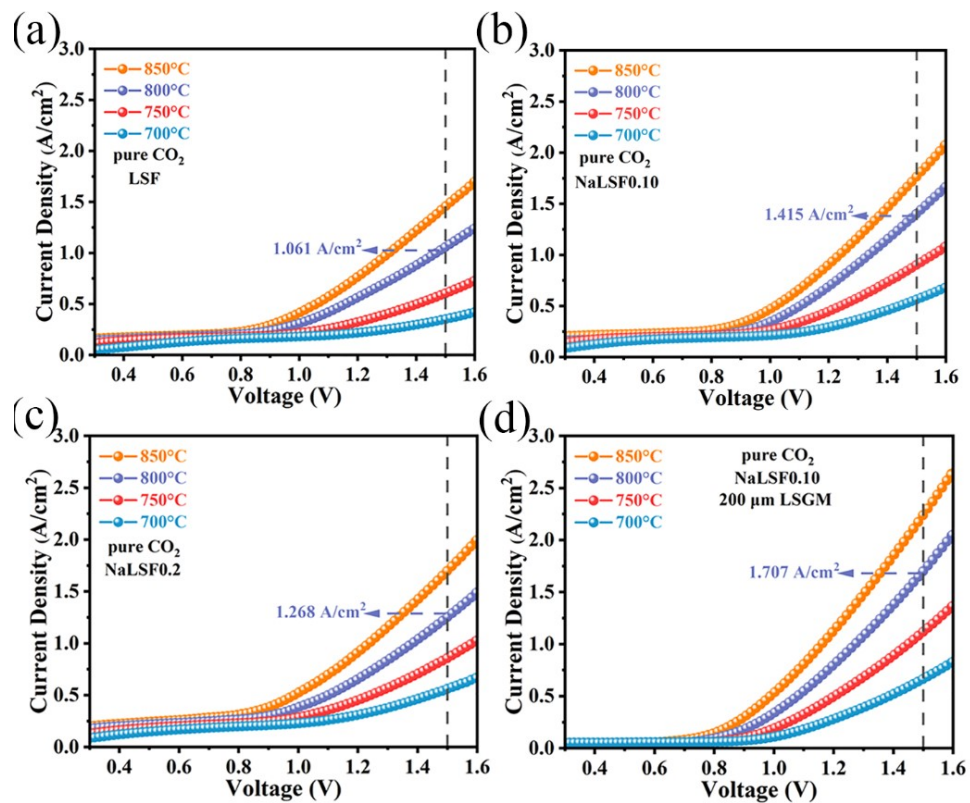


**Fig. S11.** I-V curves of SOECs with a) LSF, b) NaLSF0.10, c) NaLSF0.20, and d) NaLSF0.10 (200  $\mu m$  electrolyte) cathodes from 700 °C to 850 °C in pure  $CO_2$  atmosphere.

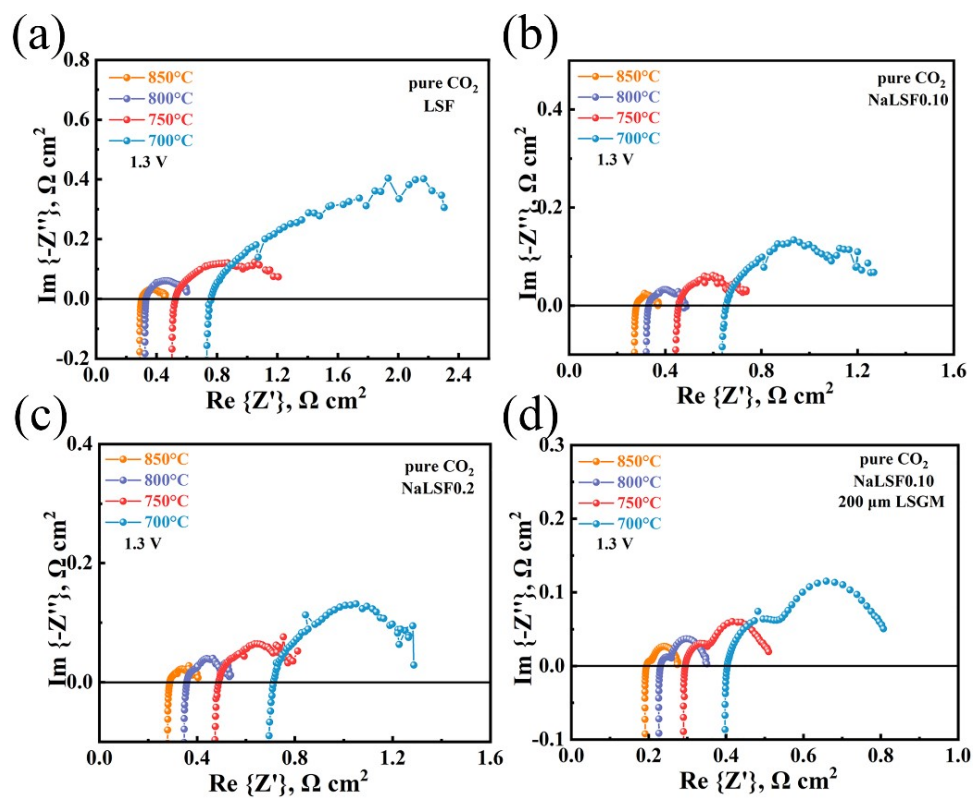


**Fig. S12.** EIS curves of SOECs with a) LSF, b) NaLSF0.10, c) NaLSF0.20, and d) NaLSF0.10 (200  $\mu\text{m}$  electrolyte) cathodes from 700  $^{\circ}\text{C}$  to 850  $^{\circ}\text{C}$  at 1.3 V in pure  $\text{CO}_2$  atmosphere.

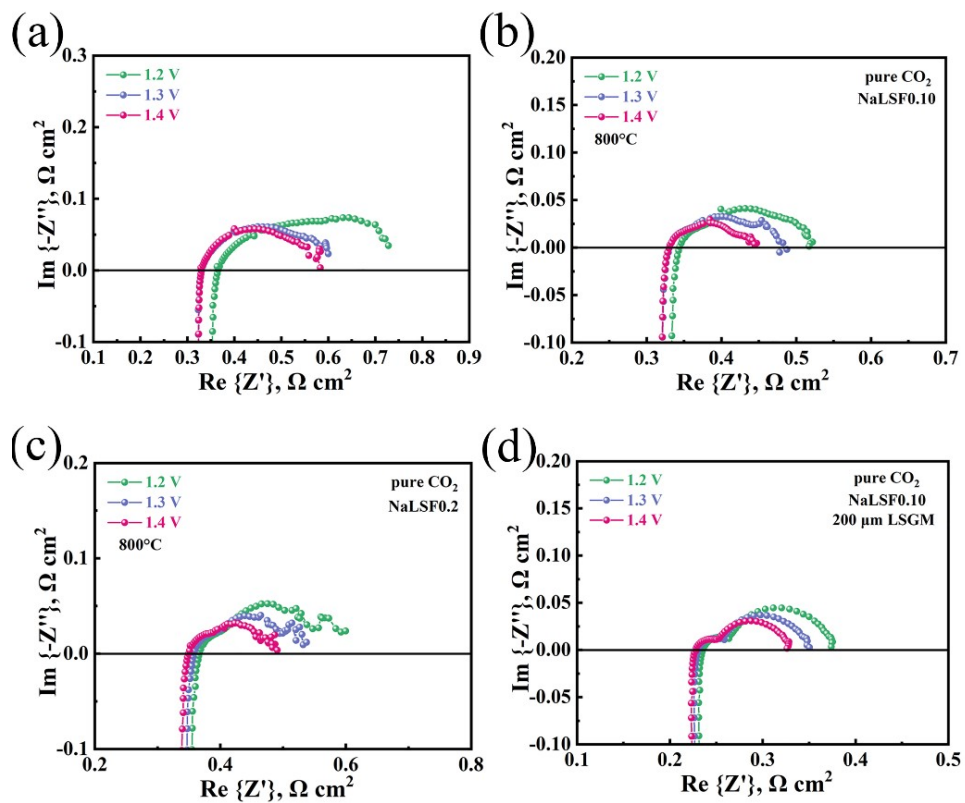


**Fig. S13.** EIS curves of SOECs with a) LSF, b) NaLSF0.10, c) NaLSF0.20, and d) NaLSF0.10 (200  $\mu\text{m}$  electrolyte) cathodes from 1.2 V to 1.4 V at 800 °C in pure  $\text{CO}_2$  atmosphere.

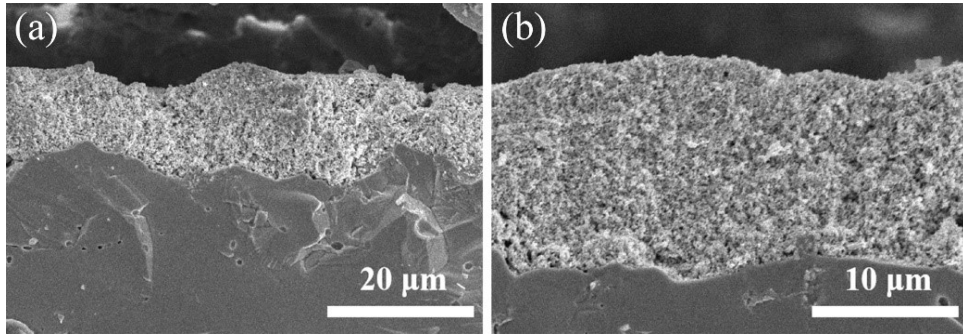


**Fig. S14.** a) and b) SEM images of the cross-sectional of SOECs with the electrolyte had been polished.

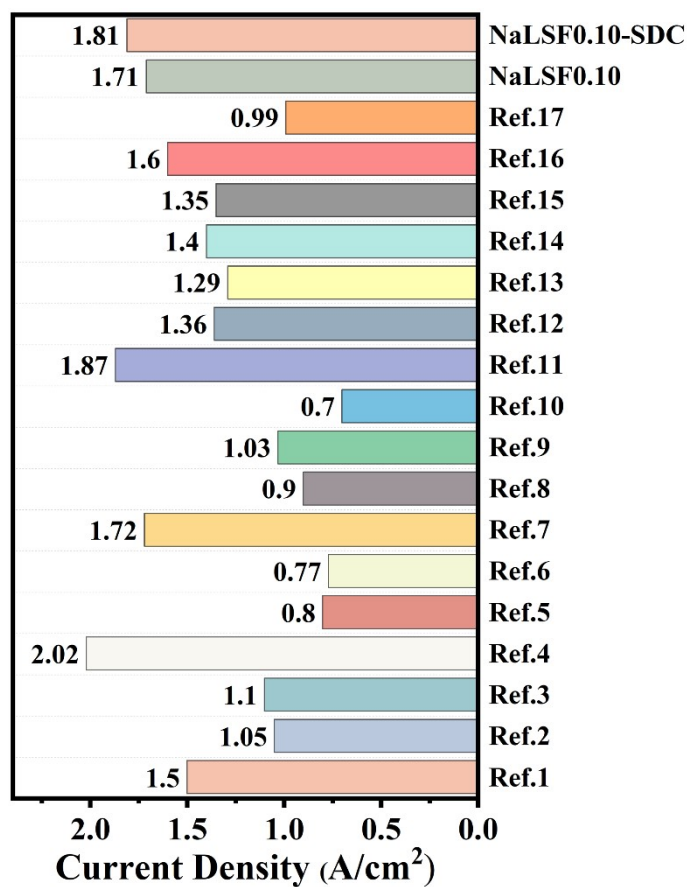


**Fig. S15.** Comparison of performance for the SOECs with NaLSF0.10 cathode in this work with reported various cathodes at 800 °C and 1.5 V.



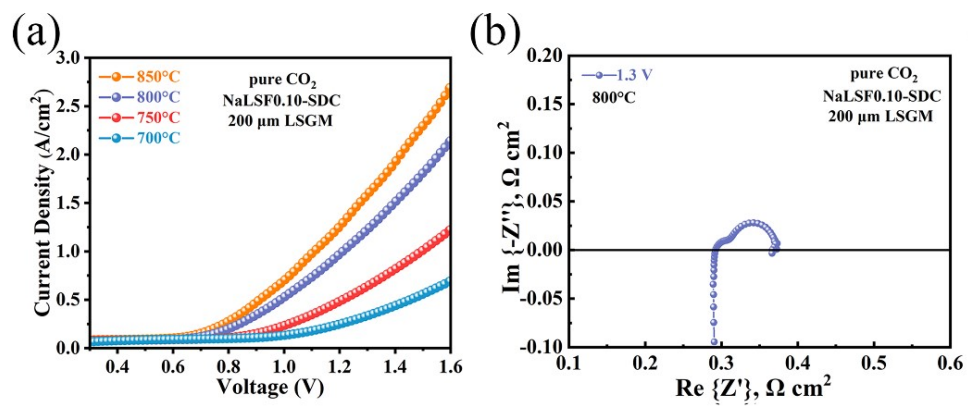


**Fig. S16.** a) I-V curves, b) EIS at 1.3 and 800 °C.

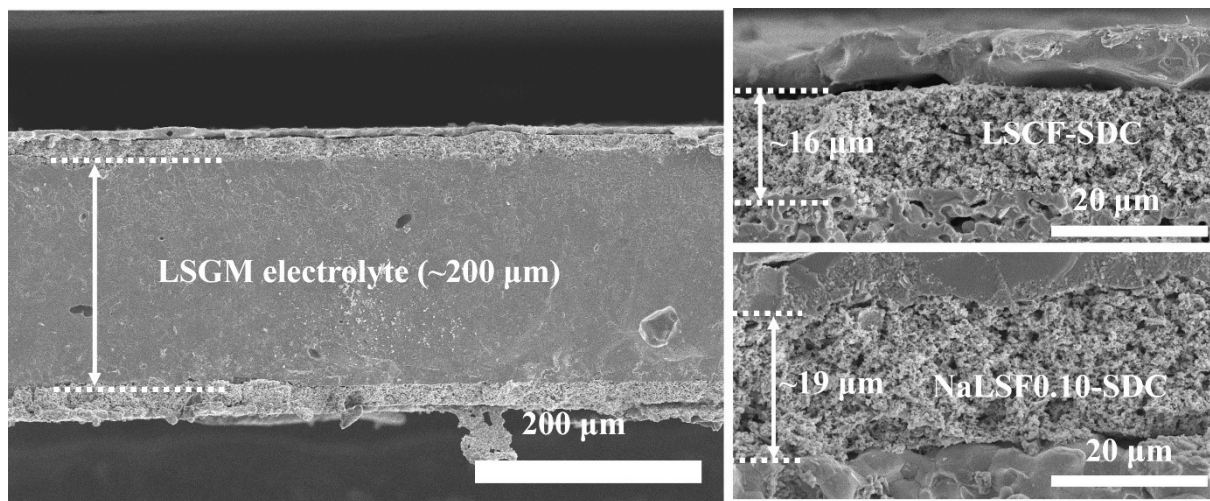


**Fig. S17.** SEM images of the cross-sectional of RSOcs after the test with NaLSF0.10-SDC cathode and LSCF-SDC anode.

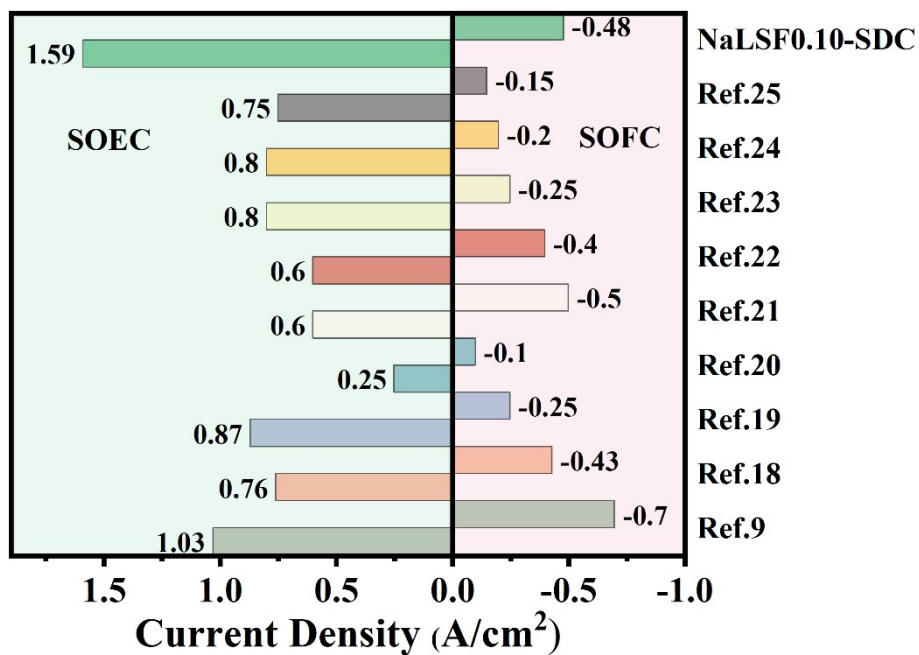


**Fig. S18.** Comparison of performance for the RSOCs with NaLSF0.10-SDC cathode in this work with reported various cathodes at 800 °C/850 °C and 1.5 V (SOEC mode) or 800 °C/850 °C and 0.6 V (SOFC mode).

**Table S1. Structural Refinement Results for LSF, NaLSF0.10, and NaLSF0.20 powders.**

	LSF	NaLSF0.10	NaLSF0.20
a (Å)	5.5252	5.5267	5.5302
b (Å)	5.5252	5.5267	5.5302
c (Å)	13.4409	13.4340	13.4434
V (Å <sup>3</sup> )	355.348	355.359	356.060
wR <sub>p</sub> (%)	8.31	8.62	8.91
R <sub>p</sub> (%)	6.62	6.67	7.00
Chi <sup>2</sup>	2.196	2.389	2.466

**Table S2. The composition of lattice oxygen and surface adsorbed oxygen species in LSF, NaLSF0.10, and NaLSF0.20 samples.**

Samples	B.E. O <i>1s</i> (eV)			O <sub>lat</sub>	O <sub>ads</sub> +O <sub>H/carbonate</sub>	O <sub>ads</sub> +O <sub>H/carbonate</sub> /O <sub>lat</sub> .
	O <sub>lat</sub>	O <sub>ads</sub>	O <sub>H/carbonate</sub>	(at.%)	(at.%)	
LSF	528.43	530.03 530.08	532.73	50.76	43.65	0.97
NaLSF0.10	528.13	529.28 530.58	531.43	35.08	48.07	1.85
NaLSF0.20	528.08	529.48 530.73	531.38	26.08	48.13	2.62

**Table S3. The composition of Fe<sup>2+</sup>, Fe<sup>3+</sup>, and Fe<sup>4+</sup> fitting by Fe 2*p* spectra in LSF, NaLSF0.10, and NaLSF0.20 samples.**

Concentration (%)	LSF	NaLSF0.10	NaLSF0.20
Fe <sup>2+</sup>	50.25	51.28	53.19
Fe <sup>3+</sup>	35.17	35.39	36.17
Fe <sup>4+</sup>	14.58	13.33	10.64

**Table S4.** Comparison of current densities for CO<sub>2</sub> electrolysis at 800 °C and 1.5 V.

Cathodes	Electrolytes//anodes	Current densities (A cm <sup>-2</sup> )	References
Sr <sub>2</sub> Fe <sub>1.5</sub> Mo <sub>0.5</sub> O <sub>3-δ</sub>	LDC/LSGM//LSCF-SDC	1.50	<i>Adv Energy Mater</i> <b>2021</b> , <i>11</i> , 2102845 <a href="#">1</a>
CoFe@Sr <sub>2</sub> Fe <sub>1.35</sub> Co <sub>0.2</sub> Mo <sub>0.45</sub> O <sub>6-δ</sub> -GDC	LDC/LSGM//BSCF-GDC	1.05	<i>Adv Mater</i> <b>2020</b> , <i>32</i> , 1906193 <a href="#">2</a>
(La <sub>0.2</sub> Sr <sub>0.8</sub> ) <sub>0.95</sub> Ti <sub>0.65</sub> Mn <sub>0.35</sub> O <sub>3-δ</sub>	LDC/LSGM//LSM	0.60	<i>Appl Catal B</i> <b>2020</b> , <i>272</i> , 118968 <a href="#">3</a>
(La <sub>0.2</sub> Sr <sub>0.8</sub> ) <sub>0.95</sub> Ti <sub>0.55</sub> Mn <sub>0.35</sub> Cu <sub>0.10</sub> O <sub>3-δ</sub>	LDC/LSGM//LSM	1.10	<i>Appl Catal B</i> <b>2020</b> , <i>272</i> , 118968 <a href="#">3</a>
CoFe-La <sub>0.4</sub> Sr <sub>0.6</sub> Co <sub>0.2</sub> Fe <sub>0.7</sub> Mo <sub>0.1</sub> O <sub>3-δ</sub>	LDC/LSGM//BSCF-GDC	2.02	<i>Angew Chem Int Ed</i> <b>2020</b> , <i>59</i> , 15968 <a href="#">4</a>
FeNi@La <sub>0.6</sub> Ca <sub>0.4</sub> Fe <sub>0.8</sub> Ni <sub>0.2</sub> O <sub>3-δ</sub>	GDC/YSZ/GDC//LSCF-GDC	0.80	<i>J Mater Chem A</i> <b>2019</b> , <i>7</i> , 6395 <a href="#">5</a>
La <sub>0.43</sub> Ca <sub>0.37</sub> Ti <sub>0.94</sub> Ni <sub>0.06</sub> O <sub>3-δ</sub> -Ce	LDC/LSGM//LSCF-GDC/LSCF	0.77	<i>J Mater Chem A</i> <b>2022</b> , <i>10</i> , 20350 <a href="#">6</a>
Ni@Sr <sub>2</sub> Fe <sub>1.5</sub> Mo <sub>0.5</sub> O <sub>6-δ</sub> -Ni@GDC	LSGM//PBSCF-GDC	1.72	<i>Appl Catal B</i> <b>2023</b> , <i>337</i> , 122968 <a href="#">7</a>
Sr <sub>2</sub> Fe <sub>1.3</sub> Zr <sub>0.2</sub> Mo <sub>0.5</sub> O <sub>6-δ</sub>	GDC//LSGM//LSCF	0.90	<i>Appl Catal B</i> <b>2022</b> , <i>317</i> , 121754 <a href="#">8</a>
Sr <sub>1.97</sub> Fe <sub>1.5</sub> Mo <sub>0.5</sub> Ni <sub>0.1</sub> O <sub>6-γ</sub>	SDC/LSGM//LSCF-SDC	1.03	<i>ACS Appl Mater. Interfaces</i> <b>2022</b> , <i>14</i> , 9138 <a href="#">9</a>
La <sub>0.5</sub> Sr <sub>0.5</sub> FeO <sub>3-δ</sub> -Pd	YSZ//LSM-YSZ	0.70	<i>Nano Energy</i> <b>2020</b> , <i>71</i> , 104598 <a href="#">10</a>
RuFe@Sr <sub>2</sub> Fe <sub>1.4</sub> Ru <sub>0.1</sub> Mo <sub>0.5</sub> O <sub>6-δ</sub> -GDC	LDC/LSGM/BSCF-GDC	1.87	<i>Nat Commun</i> , <b>2021</b> , <i>12</i> , 5665 <a href="#">11</a>
Sr <sub>2</sub> Fe <sub>1.5</sub> Mo <sub>0.5</sub> O <sub>6-δ</sub> F <sub>0.1</sub>	LDC/LSGM//LSCF-SDC	1.36	<i>Adv Energy Mater</i> <b>2019</b> , <i>9</i> , 1803156 <a href="#">12</a>
Sr <sub>2</sub> Fe <sub>1.45</sub> Ir <sub>0.05</sub> Mo <sub>0.5</sub> O <sub>6-δ</sub> -GDC	LDC/LSGM//BSCF-GDC	1.29	<i>Natl Sci Rev</i> <b>2023</b> , <i>10</i> , nwad078 <a href="#">13</a>
Sr <sub>2</sub> FeMo <sub>2/3</sub> Mg <sub>1/3</sub> O <sub>6-δ</sub>	LDC/LSGM/LDC//LSCF-SDC	1.40	<i>Nano Energy</i> <b>2021</b> , <i>82</i> , 105707 <a href="#">14</a>
La <sub>0.5</sub> Sr <sub>0.5</sub> Fe <sub>0.9</sub> Ti <sub>0.1</sub> O <sub>3-δ</sub>	LSGM//LSCF-GDC	1.35	<i>Ceram Inter</i> <b>2022</b> , <i>48</i> , 4223 <a href="#">15</a>
La <sub>0.55</sub> Sr <sub>0.45</sub> Fe <sub>0.9</sub> Mo <sub>0.1</sub> O <sub>3-δ</sub>	LSGM//LSC	1.60	<i>Chem Eng J</i> <b>2022</b> , <i>433</i> , 133632 <a href="#">16</a>
La <sub>0.6-x</sub> Li <sub>x</sub> Sr <sub>0.4</sub> Co <sub>0.7</sub> Mn <sub>0.3</sub> O <sub>3-δ</sub>	LSGM//LSCF	0.99	<i>Small</i> <b>2023</b> , 2303305 <a href="#">17</a>
Ce <sub>0.9</sub> M <sub>0.1</sub> O <sub>2-δ</sub> infiltrated LSCrF-GDC	YSZ//LSM-YSZ	0.60	<i>J Energy Chem</i> <b>2020</b> , <i>40</i> , 46 <a href="#">18</a>
(La <sub>4</sub> Sr <sub>4</sub> ) <sub>0.9</sub> Ti <sub>7.2</sub> Ni <sub>0.8</sub> O <sub>26</sub>	YSZ//LSCF	1.20	<i>J Energy Chem</i> <b>2023</b> , <i>84</i> , 219 <a href="#">19</a>
Sr <sub>2</sub> Fe <sub>1.4</sub> Zn <sub>0.1</sub> Mo <sub>0.5</sub> O <sub>6-δ</sub>	LSGM/BSCF	~1.50	<i>Green Chem</i> <b>2023</b> , DOI: 10.1039/D3GC03518B <a href="#">20</a>
NaLSF0.10	LSGM//LSCF-SDC	1.71	<b>This work</b>
NaLSF0.10-SDC	LSGM//LSCF-SDC	1.81	

GDC: Gd<sub>0.2</sub>Ce<sub>0.8</sub>O<sub>2-δ</sub>; LDC: La<sub>0.4</sub>Ce<sub>0.8</sub>O<sub>2-δ</sub>; SDC: Sm<sub>0.2</sub>Ce<sub>0.8</sub>O<sub>2-δ</sub>; LSM: La<sub>0.8</sub>Sr<sub>0.2</sub>MnO<sub>3-δ</sub>; LSCF: La<sub>0.6</sub>Sr<sub>0.4</sub>Co<sub>0.2</sub>Fe<sub>0.8</sub>O<sub>3-δ</sub>; YSZ (8% nickel-yttria stabilized zirconia), BSCF: Ba<sub>0.5</sub>Sr<sub>0.5</sub>Co<sub>0.8</sub>Fe<sub>0.2</sub>O<sub>3-δ</sub>, PBSCF: PrBa<sub>0.5</sub>Sr<sub>0.5</sub>Co<sub>1.5</sub>Fe<sub>0.5</sub>O<sub>5+δ</sub>.

**Table S5.** Comparison of performance of RSOCs for CO-CO<sub>2</sub> at 800 °C and 1.5 V.

Fuel electrode	Electrolytes//air electrode	Current densities (A cm <sup>-2</sup> )		References
		SOEC@1.5V	SOFC@0.6V	
Sr <sub>1.97</sub> Fe <sub>1.5</sub> Mo <sub>0.5</sub> Ni <sub>0.1</sub> O <sub>6-γ</sub>	YSZ//SDC//LSCF	1.03	0.70	<i>ACS Appl Mater. Interfaces</i> <b>2022</b> , <i>14</i> ,
Ni-YSZ (70% CO-CO <sub>2</sub> )		0.91	0.95	9138
CoFe-Sr <sub>2</sub> Fe <sub>7/6</sub> Mo <sub>0.5</sub> Co <sub>1/3</sub> O <sub>6-δ</sub> in 2:1 CO-CO <sub>2</sub>	SDC/YSZ//LSM-SDC	0.76	0.43	<i>Sci China Mater</i> <b>2021</b> <i>64</i> , 1114
La <sub>0.6</sub> Sr <sub>0.4</sub> Fe <sub>0.8</sub> Ni <sub>0.2</sub> O <sub>3-δ</sub> -GDC in 30% CO-CO <sub>2</sub>	YSZ/GDC//LSCF-GDC	0.87	0.25	<i>J Mater Chem A</i> <b>2017</b> , <i>5</i> , 2673
La <sub>0.3</sub> Sr <sub>0.7</sub> Fe <sub>0.7</sub> Ti <sub>0.3</sub> O <sub>3-δ</sub> in 30% CO-CO <sub>2</sub>	SDC/YSZ/SDC//La <sub>0.3</sub> Sr <sub>0.7</sub> Fe <sub>0.7</sub> Ti <sub>0.3</sub> O <sub>3</sub>	0.25	0.10	<i>Electrochimica Acta</i> <b>2020</b> , <i>332</i> , 135464
FeNi@La <sub>0.6</sub> Sr <sub>0.4</sub> Fe <sub>0.8</sub> Ni <sub>0.2</sub> O <sub>3-δ</sub> -GDC	GDC/YSZ/GDC//LSCF-GDC	0.60	0.50	<i>ACS Catalysis</i> <b>2016</b> , <i>6</i> , 6219-6228
Sr <sub>2</sub> Fe <sub>1.5</sub> Mo <sub>0.5</sub> O <sub>6-δ</sub> -YSZ	YSZ//SFM-YSZ	0.60	0.40	<i>Solid State Ionics</i> , <b>2018</b> , <i>319</i> 98-104
CoFe@Pr <sub>0.4</sub> Sr <sub>0.6</sub> Co <sub>0.2</sub> Fe <sub>0.7</sub> Mo <sub>0.1</sub> O <sub>3-δ</sub> -GDC in 30% CO-CO <sub>2</sub>	GDC/YSZ/GDC//LSCF-GDC	0.80 (850°C)	0.25 (850°C)	<i>J Mater Chem A</i> <b>2016</b> , <i>5</i> , 2673
Pr <sub>0.4</sub> Sr <sub>0.6</sub> Co <sub>0.2</sub> Fe <sub>0.7</sub> Mo <sub>0.1</sub> O <sub>3-δ</sub> -GDC in 30% CO-CO <sub>2</sub>		0.65 (850°C)	0.14 (850°C)	
Co@La <sub>0.6</sub> Sr <sub>0.4</sub> Co <sub>0.7</sub> Mn <sub>0.3</sub> O <sub>3</sub> in 30% CO-CO <sub>2</sub>	GDC/LSGM//LSCF-GDC	0.80	0.20	<i>Appl Catal B</i> <b>2019</b> , <i>272</i> , 147-156
CoNi@La <sub>0.6</sub> Sr <sub>0.4</sub> Co <sub>0.5</sub> Ni <sub>0.2</sub> Mn <sub>0.3</sub> O <sub>3</sub>	GDC/LSGM//LSCF-GDC	0.75	0.15	<i>J Mater Chem A</i> <b>2020</b> , <i>8</i> , 138
NaLSF0.10-SDC	LSGM//LSCF-SDC	1.59	0.48	<b>This work</b>

Noted, if not specific statement, the applied fuel electrode gas atmosphere is 50% CO-CO<sub>2</sub>



## References

1. X. Xi, J. Liu, W. Luo, Y. Fan, J. Zhang, J. Luo and X. Fu, *Adv. Energy Mater.*, 2021, **11**, 2102845.
2. H. Lv, L. Lin, X. Zhang, Y. Song, H. Matsumoto, C. Zeng, N. Ta, W. Liu, D. Gao, G. Wang and X. Bao, *Adv. Mater.*, 2020, **32**, e1906193.
3. X. Yang, K. Sun, M. Ma, C. Xu, R. Ren, J. Qiao, Z. Wang, S. Zhen, R. Hou and W. Sun, *Appl. Catal. B*, 2020, **272**, 118968.
4. H. Lv, T. Liu, X. Zhang, Y. Song, H. Matsumoto, N. Ta, C. Zeng, G. Wang and X. Bao, *Angew. Chem. Int. Ed.*, 2020, **59**, 15968-15973.
5. Y. Tian, L. Zhang, Y. Liu, L. Jia, J. Yang, B. Chi, J. Pu and J. Li, *J. Mater. Chem. A*, 2019, **7**, 6395-6400.
6. Z. Li, M. Peng, Y. Zhu, Z. Hu, C. Pao, Y. Chang, Y. Zhang, Y. Zhao, J. Li and Y. Sun, *J. Mater. Chem. A*, 2022, **10**, 20350-20364.
7. F. Hu, Y. Ling, S. Fang, L. Sui, H. Xiao, Y. Huang, S. Wang, B. He and L. Zhao, *Appl. Catal. B*, 2023, **337**, 122968.
8. L. Zhang, W. Sun, C. Xu, R. Ren, X. Yang, J. Qiao, Z. Wang, S. Zhen and K. Sun, *Appl. Catal. B*, 2022, **317**, 121754.
9. Y. Li, Y. Li, S. Zhang, C. Ren, Y. Jing, F. Cheng, Q. Wu, P. Lund and L. Fan, *ACS Appl. Mater. Interfaces*, 2022, **14**, 9138-9150.
10. Y. Zhou, L. Lin, Y. Song, X. Zhang, H. Lv, Q. Liu, Z. Zhou, N. Ta, G. Wang and X. Bao, *Nano Energy*, 2020, **71**, 104598.
11. H. Lv, L. Lin, X. Zhang, R. Li, Y. Song, H. Matsumoto, N. Ta, C. Zeng, Q. Fu, G. Wang and X. Bao, *Nat. Commun.*, 2021, **12**, 5665.
12. Y. Li, Y. Li, Y. Wan, Y. Xie, J. Zhu, H. Pan, X. Zheng and C. Xia, *Adv. Energy Mater.*, 2019, **9**, 1803156.
13. Y. Shen, T. Liu, R. Li, H. Lv, N. Ta, X. Zhang, Y. Song, Q. Liu, W. Feng, G. Wang and X. Bao, *Natl. Sci. Rev.*, 2023, **10**, nwad078.
14. X. Xi, J. Liu, Y. Fan, L. Wang, J. Li, M. Li, J. Luo and X. Fu, *Nano Energy*, 2021, **82**, 105707.
15. Y. Hou, L. Wang, L. Bian, Q. Zhang, L. Chen and K.-c. Chou, *Ceram. Int.*, 2022, **48**, 4223-4229.

16. D. He, W. Ruan, J. Li, J. Ni and C. Ni, *Chem. Eng. J.*, 2022, **433**, 133632.
17. W. Lin, W. Su, Y. Li, T. Chiu, M. Singh, Z. Pan and L. Fan, *Small*, 2023, **19**, 2303305.
18. Z. Huang, Z. Zhao, H. Qi, X. Wang, B. Tu and M. Cheng, *J. Energy Chem.*, 2020, **40**, 46-51.
19. Z. Liu, J. Zhou, Y. Sun, X. Yue, J. Yang, L. Fu, Q. Deng, H. Zhao, C. Yin and K. Wu, *J. Energy Chem.*, 2023, **84**, 219-227.
20. S. Liu, M. Yang, R. Xu, X. Xiang, G. Yang, H. Xu, G. Xiao, R. Ran, W. Zhou and Z. Shao, *Green Chem.*, 2023, 10.1039/D3GC03518B.
21. Y. Li, M. Singh, Z. Zhuang, Y. Jing, F. Li, K. Maliutina, C. He and L. Fan, *Sci. China Mater.*, 2021, **64**, 1114-1126.
22. S. Liu, Q. Liu and J.-L. Luo, *Journal of Materials Chemistry A*, 2017, **5**, 2673-2680.
23. Z. Cao, Z. Wang, F. Li, K. Maliutina, Q. Wu, C. He, Z. Lv and L. Fan, *Electrochim. Acta*, 2020, **332**, 135464.
24. S. Liu, Q. Liu and J.-L. Luo, *ACS Catalysis*, 2016, **6**, 6219-6228.
25. Y. Li, S. Zou, J. Ju and C. Xia, *Solid State Ion.*, 2018, **319**, 98-104.
26. S. Liu, Q. Liu and J.-L. Luo, *Journal of Materials Chemistry A*, 2016, **4**, 17521-17528.
27. S. Park, Y. Kim, H. Han, Y. Chung, W. Yoon, J. Choi and W. Kim, *Appl. Catal. B*, 2019, **248**, 147-156.
28. S. Park, Y. Kim, Y. Noh, T. Kim, H. Han, W. Yoon, J. Choi, S.-H. Yi, W.-J. Lee and W. B. Kim, *Journal of Materials Chemistry A*, 2020, **8**, 138-148.